

Feature article

DNA interaction and antimicrobial activity of novel tetradentate imino-oxalato mixed ligand metal complexes



Narayanaperumal Pravin, Natarajan Raman*

Research Department of Chemistry, VHNSN College, Virudhunagar 626 001, India

ARTICLE INFO

Article history:

Received 29 May 2013

Accepted 10 August 2013

Available online 17 August 2013

Keywords:

Mixed-ligand complexes

Calf thymus DNA

Intercalation

pBR322 DNA

MIC data

ABSTRACT

Four novel DNA metalloinsertors having imino-oxalato mixed-ligands, of the composition $[ML(ox)]Cl_2$ (where $M = Cu(II), Co(II), Ni(II)$ and $Zn(II)$; $ox = C_2O_4^{2-}$ and $L = N,N'$ -bis(4-chlorobenzylidene)benzene-1,2-diamine) were synthesized. They were fully characterized by microanalytical data, magnetic susceptibility values, molar conductivity measurements, UV–vis, IR, 1H NMR, ^{13}C NMR and EPR techniques. Their geometry was explored and found to have square-planar geometry. Electronic absorption spectroscopy, cyclic voltammetry and viscosity measurements indicate that these mixed-ligand complexes strongly bind to calf thymus DNA, presumably via an intercalation mechanism. Further, DNA cleavage efficacy of these complexes was investigated by gel electrophoresis. The complexes were found to promote the cleavage of pBR322 DNA in the presence of the reluctant, ascorbic acid. The ligand (L) and the mixed-ligand complexes were tested for their efficiency towards antimicrobial activity and their MIC data reveal that all the complexes have strong activity in comparison to the free ligand and standard drugs, ciprofloxacin and fluconazole.

© 2013 Elsevier B.V. All rights reserved.

Contents

Acknowledgments	49
Appendix A. Supplementary material	49
References	49

There is an increasing prominence and evergreen budding curiosity in the field of metal-containing drugs, and medicinal inorganic chemistry covering wide applications of metals in therapeutics and diagnostics [1]. A major advantage of these metal-based over organic-based drugs is their ability to vary coordination number, geometry and redox states. Metals can also alter the pharmacological properties of organic based drugs by forming coordination compounds with them [2]. In topical years, the metal complexes with chelating ligands bearing O, N type donor atoms of alternative organic structures have attracted the chemists owing to their interesting medicinal applications [3]. Their mixed-ligand metal complexes are of special interest because of their variance in ways in which they are bonded to metal ions [4]. Further, it is also known that Schiff bases belong to a class of organic compounds possessing anti-cancer potential as their activity can be increased when they complex with metal ions [5,6].

The interaction of metal complexes containing N_2 type Schiff base ligands has been thoroughly considered [7–9]. DNA binding is the critical step for DNA activity. To design effective chemotherapeutic agents and better anticancer drugs, it is essential to explore the interaction of metal complexes with DNA. In recent years, attention has been devoted to the mixed ligand complexes of transition metals containing nitrogen donors [10–12] with potential applications as herbicidal [12–14], antibacterial [15–17], antitumor [18,19], antiviral [20] and antifungal [21] agents.

Accordingly we intend to report herein, the synthesis of metal complexes with nitrogen donor Schiff bases (*p*-substituted aldehyde and *o*-phenylenediamine) as primary ligand and oxalic acid as co-ligand. Besides the characterization of complexes was carried out by physicochemical techniques like IR, UV–vis, NMR, EPR, elemental analyses, magnetic susceptibility, conductance measurements and the role of functional groups on the binding mode was evaluated (Scheme 1).

The Schiff base ligand and its mixed ligand complexes were prepared by a typical procedure [22–28]. The materials and methods for the newly synthesized mixed-ligand complexes and their characterization were depicted as S1 and S2 (Supplementary files). We acquired the

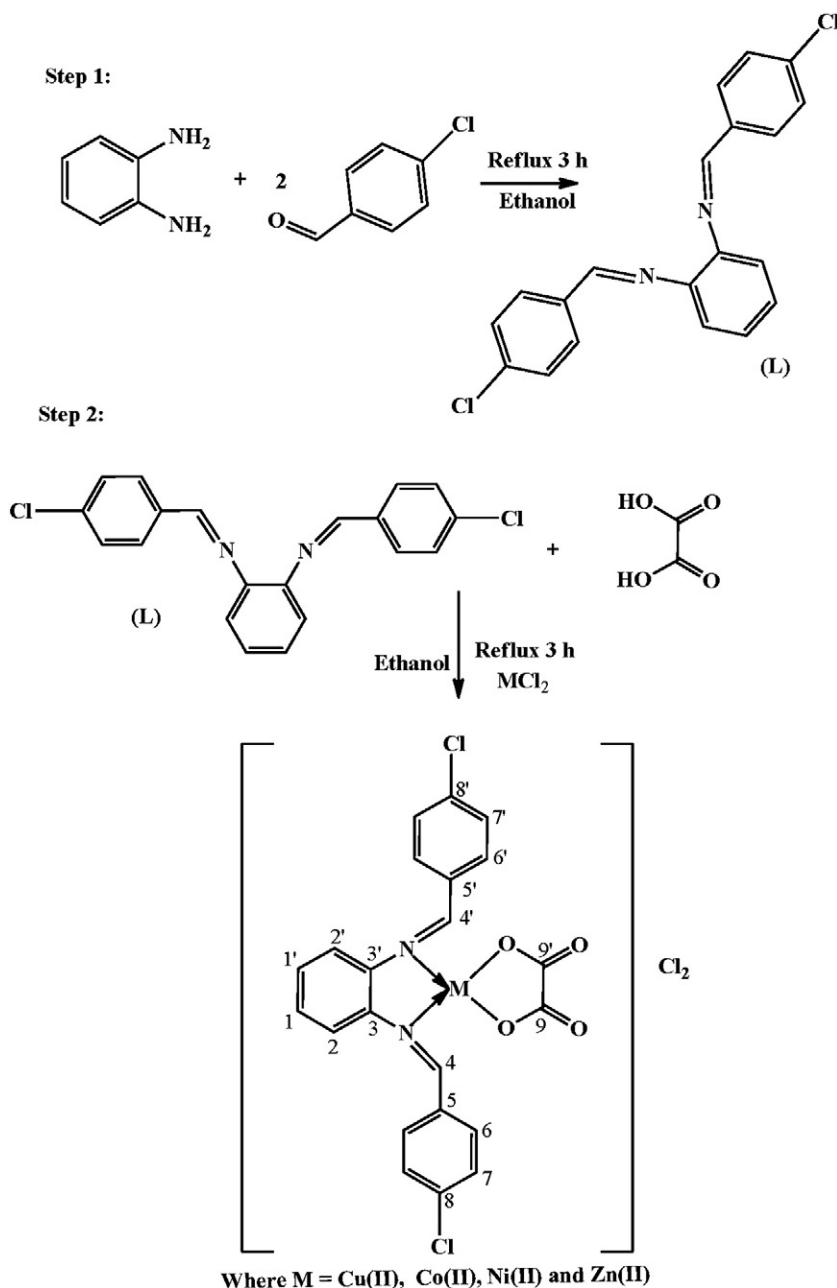
* Corresponding author. Tel.: +91 92451 65958; fax: +91 4562 281338.

E-mail address: drm_raman@yahoo.co.in (N. Raman).

probable composition of complexes as $[ML(ox)]Cl_2$ (where $M = Cu(II), Co(II), Ni(II)$ and $Zn(II)$; $ox = C_2O_4^{2-}$ and $L = N,N'$ -bis(4-chlorobenzylidene)benzene-1,2-diamine) which were confirmed through elemental analyses, magnetic susceptibility, NMR, UV, IR, EPR spectra and molar conductivity measurements since no single crystals suitable for X-ray determination could be isolated.

The representative absorption spectra of $Cu(II)$ complex in presence and absence of CT-DNA are shown in Fig. 1. The absorption spectra of other complexes are given in supplementary file (Fig. S1 to S3). The binding mode of complexes to CT-DNA helix has been followed through absorption spectral titrations. With increasing concentration of CT-DNA the absorption bands of the complexes were affected resulting in the tendency of hypochromism and a minor red shift was observed in all the complexes. Hyperchromic effect and hypochromic effect are the spectral features of DNA concerning its double helix structure. Hypochromism results from the contraction of DNA in the helix axis as well as from the change in conformation on DNA while hyperchromism results from the

damage of the DNA double helix structure [29]. The absorption spectra of $Cu(II), Co(II), Ni(II)$ and $Zn(II)$ complexes exhibited intensive absorption bands at 376.2, 343.0, 310.8 and 399.8 nm respectively in 5 mM Tris-HCl and 50 mM NaCl buffer solution (pH 7.2). On increasing the concentration of CT DNA resulted in the red shift in the range 3.1, 2.2, 1.9 and 1.3 nm and significant hypochromicity lying in the range 41.3%, 29.1%, 32.5% and 24.1%. The K_b values are shown in Table 1. The intrinsic binding constant values (K_b) for the complexes $Cu(II), Co(II), Ni(II)$ and $Zn(II)$ are found to be $3.1 \pm 0.05 \times 10^5, 2.2 \pm 0.08 \times 10^5, 1.9 \pm 0.04 \times 10^5$ and $1.3 \pm 0.12 \times 10^5 M^{-1}$ respectively. These spectral characteristics may suggest an intercalative mode of binding which involves a stacking interaction between the aromatic chromophore and the DNA base pairs. The binding constant (K_b) values of these complexes are lower in comparison to those observed for typical intercalators, ethidium bromide and $[Ru(bpy)_2(dppz)]^{2+}$ whose binding constants are in the order of 1.4×10^6 and $>10^6 M^{-1}$ [30,31]. The results suggest that the interaction of four metal complexes with DNA is a moderate intercalative mode.



Scheme 1. The schematic representation for the synthesis and structure of Schiff base (L) and its mixed-ligand metal complexes.

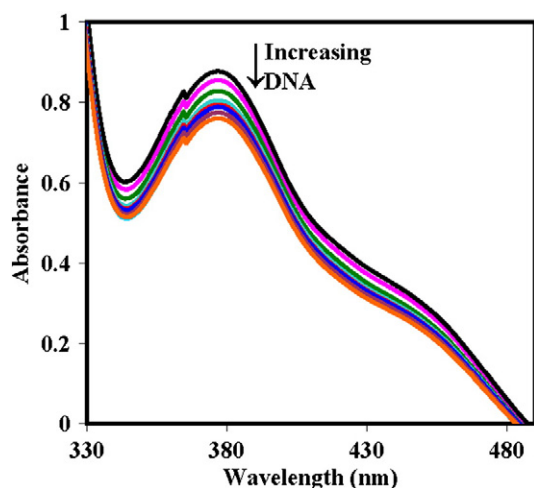


Fig. 1. Absorption spectral changes on addition of CT DNA to the solution of $[\text{CuL}(\text{ox})]\text{Cl}_2$ in buffer pH = 7.2 at 25 °C in the presence of increasing amount of DNA. Arrow indicates the changes in absorbance upon increasing the DNA concentration.

The cyclic voltammograms of the copper complex in the absence and presence of different amounts of DNA are shown in Fig. 2. In the absence of CT DNA, the first redox cathodic peak appeared at -0.156 V for $\text{Cu}(\text{III}) \rightarrow \text{Cu}(\text{II})$ ($E_{\text{p}_a} = 0.426$ V, $E_{\text{p}_c} = -0.156$ V, $\Delta E_{\text{p}} = 0.452$ V, and $E_{1/2} = 0.134$ V). In the second redox couple, the cathodic peak appeared at -0.408 V for $\text{Cu}(\text{II}) \rightarrow \text{Cu}(\text{I})$ ($E_{\text{p}_a} = 0.154$ V, $E_{\text{p}_c} = -0.408$ V, $\Delta E_{\text{p}} = 0.507$ V, and $E_{1/2} = -0.149$ V) and in the third redox couple, the cathodic peak appeared at -0.836 V for $\text{Cu}(\text{I}) \rightarrow \text{Cu}(\text{0})$ ($E_{\text{p}_a} = 0.008$ V, $E_{\text{p}_c} = -0.836$ V, $\Delta E_{\text{p}} = 0.554$ V, and $E_{1/2} = -0.335$ V). The $I_{\text{p}_a}/I_{\text{p}_c}$ ratios for these three redox couples are 1.3, 1.4, and 1.1, respectively, which indicate that reaction of the complex on the glassy carbon electrode surface is a quasi-reversible redox process. During the incremental addition of CT DNA to the complex, the redox couples caused a positive shift in $E_{1/2}$ and decrease of ΔE_{p} (Table 2). The $I_{\text{p}_a}/I_{\text{p}_c}$ values were also decreased in the presence of DNA.

The cyclic voltammogram of $[\text{NiL}(\text{ox})]\text{Cl}_2$ in the absence of CT-DNA featured two anodic peaks ($E_{\text{p}_a} = 0.007$ V, $E_{\text{p}_{a2}} = 0.272$ V) and two cathodic peaks ($E_{\text{p}_{c1}} = 0.411$ V, $E_{\text{p}_{c2}} = -0.178$ V). The oxidation of peak $E_{\text{p}_{a1}}$ referred to $\text{Ni}(\text{I})/\text{Ni}(\text{II})$, and the reduction of $\text{Ni}(\text{II})$ occurred at -0.411 V upon reversing the scan direction. The anodic and cathodic peak potentials were separated by 0.421 V, and the ratio of the anodic to cathodic peak currents, $I_{\text{p}_a}/I_{\text{p}_c} = 1.35$, indicating a quasi-reversible redox process. The oxidation of peak E_{p_a} referred to $\text{Ni}(\text{II})/\text{Ni}(\text{III})$, and reduction of $\text{Ni}(\text{II})$ occurred at -0.178 V upon reversing the scan direction. The anodic and cathodic peak potentials were separated by 0.453 V, and the ratio of the anodic to cathodic peak currents, $I_{\text{p}_a}/I_{\text{p}_c} = 1.08$, indicating a quasi-reversible redox process. The formal potentials $E_{1/2}$, taken as the average of E_{p_a} and E_{p_c} are -0.202 and 0.094 V. For $\text{Co}(\text{III}) \rightarrow \text{Co}(\text{II})$, the redox couple cathodic peak appeared at 0.105 in the absence of CT-DNA ($E_{\text{p}_a} = 0.365$ V, $E_{\text{p}_c} = 0.123$ V, $\Delta E_{\text{p}} = 0.242$ V, and $E_{1/2} = -0.239$ V). It was noted that the ratio $I_{\text{p}_a}/I_{\text{p}_c}$ was approximately unity. This indicates that the reaction

Table 1
Electronic absorption spectral properties of $\text{Cu}(\text{II})$, $\text{Co}(\text{II})$, $\text{Ni}(\text{II})$ and $\text{Zn}(\text{II})$ complexes.

Complex	λ_{max}		$\Delta\lambda$ (nm)	H% ^a	$K_{\text{b}} \times 10^5$ (M^{-1}) ^b
	Free	Bound			
$[\text{CuL}(\text{ox})]\text{Cl}_2$	376.2	377.8	1.6	41.3	3.1 ± 0.05
$[\text{CoL}(\text{ox})]\text{Cl}_2$	343.0	345.5	2.5	29.1	2.2 ± 0.08
$[\text{NiL}(\text{ox})]\text{Cl}_2$	310.8	313.1	2.3	32.5	1.9 ± 0.04
$[\text{ZnL}(\text{ox})]\text{Cl}_2$	351.5	353.4	1.9	24.1	1.3 ± 0.12

^a H% = $[(A_{\text{free}} - A_{\text{bound}}) / A_{\text{free}}] \times 100\%$.

^b K_{b} = Intrinsic DNA binding constant determined from the UV-vis absorption spectral titration.

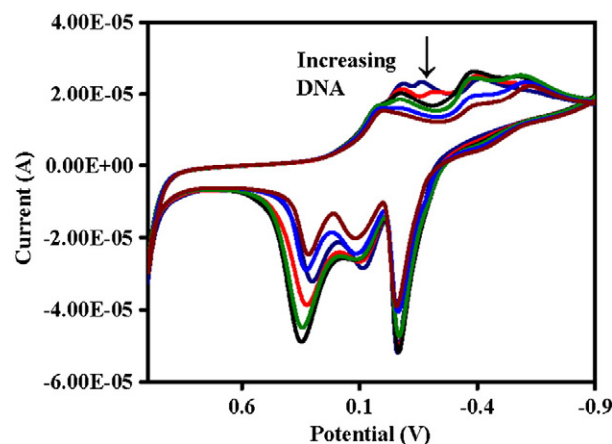


Fig. 2. Cyclic voltammogram of $[\text{CuL}(\text{ox})]\text{Cl}_2$ in the presence of increasing amount of DNA in buffer pH = 7.2 at 25 °C. Arrow indicates the changes in voltammetric currents upon increasing the DNA concentration.

of the complex on the glassy carbon electrode surface is a quasi-reversible redox process. The incremental addition of CT-DNA to the complex caused a positive shift in the formal potential ($E_{1/2}$), indicating that $[\text{CoL}(\text{ox})]\text{Cl}_2$ has bonded favorably with DNA via intercalation.

A quasi-reversible transfer process with the redox couple $[\text{Zn}(\text{II}) \rightarrow \text{Zn}(\text{0})]$ was observed for the $\text{Zn}(\text{II})$ complex. The cathodic peak appeared at -0.532 V in the absence of DNA ($E_{\text{p}_a} = -0.065$ V, $E_{\text{p}_c} = -0.532$ V, $\Delta E_{\text{p}} = 0.504$ V, and $E_{1/2} = -0.158$ V). The $I_{\text{p}_a}/I_{\text{p}_c}$ ratio is 0.93. This indicates the quasi-reversible redox process of the metal complex. Incremental addition of DNA to the $\text{Zn}(\text{II})$ complex resulted in a slight decrease in the current intensity and negative shift of the oxidation peak potential. The resulting minor changes in the current and potential are indicative of diffusion of the metal complexes bound to the large, slowly diffusing DNA molecule [32]. Electrochemical data for the $\text{Cu}(\text{II})$, $\text{Co}(\text{II})$, $\text{Ni}(\text{II})$, and $\text{Zn}(\text{II})$ complexes are shown in Table 2.

Further clarification of the interaction mode between the copper complex and DNA has been carried out by viscosity measurements. Hydrodynamic measurements that are sensitive to length change (i.e. viscosity and sedimentation) are regarded as the least ambiguous and the most critical tests of the binding mode in solution in the absence of crystallographic structural data [33]. The electrostatic binding mode has no obvious effect on the viscosity of DNA, while, a classical intercalation mode will result in lengthening the DNA helix as the base pairs are separated to accommodate the bound intercalators, leading to the increase of DNA viscosity [34]. The effect of the copper(II) complex on the relative viscosity of DNA is shown in Fig. 3. The plots of $(\eta/\eta^0)^{1/3}$ versus $[\text{Complex}] / [\text{DNA}] = R$ give a measure of the viscosity changes (Fig. 3). For comparison, the free ligand on the relative viscosity of DNA was also investigated. It was found that the free ligand was not

Table 2
Electrochemical parameters for the interaction of DNA with $\text{Cu}(\text{II})$, $\text{Co}(\text{II})$, $\text{Ni}(\text{II})$ and $\text{Zn}(\text{II})$ complexes.

Complex	Redox couple	$E_{1/2}(\text{V})^a$		$\Delta E_{\text{p}}(\text{V})^b$		$I_{\text{p}_a}/I_{\text{p}_c}$
		Free	Bound	Free	Bound	
$[\text{CuL}(\text{ox})]\text{Cl}_2$	$\text{Cu}(\text{III}) \rightarrow \text{Cu}(\text{II})$	0.134	0.126	0.452	0.434	1.32
	$\text{Cu}(\text{II}) \rightarrow \text{Cu}(\text{I})$	-0.149	-0.121	0.491	0.507	1.41
	$\text{Cu}(\text{I}) \rightarrow \text{Cu}(\text{0})$	-0.335	-0.336	0.554	0.551	1.12
$[\text{NiL}(\text{ox})]\text{Cl}_2$	$\text{Ni}(\text{III}) \rightarrow \text{Ni}(\text{II})$	0.096	0.075	0.453	0.466	1.08
	$\text{Ni}(\text{II}) \rightarrow \text{Ni}(\text{I})$	-0.206	-0.189	0.421	0.405	1.35
$[\text{CoL}(\text{ox})]\text{Cl}_2$	$\text{Co}(\text{III}) \rightarrow \text{Co}(\text{II})$	-0.239	0.254	0.241	0.242	1.16
	$[\text{ZnL}(\text{ox})]\text{Cl}_2$	$\text{Zn}(\text{II}) \rightarrow \text{Zn}(\text{0})$	-0.158	0.176	0.504	0.527

^a Data from cyclic voltammetric measurements; $E_{1/2}$ is calculated as average of anodic (E_{p_a}) and (E_{p_c}) peak potential $E_{1/2} = E_{\text{p}_a} + E_{\text{p}_c} / 2$.

^b $\Delta E_{\text{p}} = E_{\text{p}_a} - E_{\text{p}_c}$.

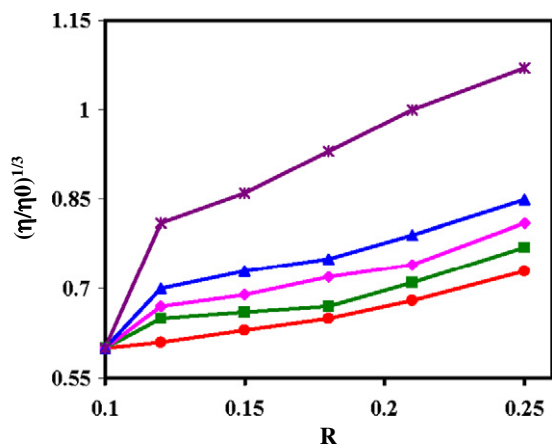


Fig. 3. Effect of increasing amounts of $[\text{CuL}(\text{ox})]\text{Cl}_2$ (■), $[\text{CoL}(\text{ox})]\text{Cl}_2$ (◆), $[\text{NiL}(\text{ox})]\text{Cl}_2$ (▲), $[\text{ZnL}(\text{ox})]\text{Cl}_2$ (●) on the viscosity of DNA and [EB] (*).

an obvious influence on the relative viscosity of DNA, suggesting the absence of intercalation of between the two species. However, when the copper(II) complex was added, the relative viscosity of DNA increased gradually, which is typical characteristic of intercalation. The classical intercalators like ethidium bromide are known to increase the base pair separation resulting in an increase in the relative viscosity of the DNA. This effect of the metal(II) complexes is far less than that observed for an intercalator such as EB indicating that there exists a moderate intercalative interaction between the complexes and CT DNA. These results also suggest that the coordination geometry has great impact on the binding mode of the small molecules with DNA. Compared with the free ligand, the copper complex has a larger rigid planar structure, which is more favorable for intercalation into DNA. Meanwhile, the negative charge of the free ligand is neutralized by coordinating with Cu(II) ion, reducing the electrostatic repulse of the molecule to DNA.

The presence of bioactive ligand and DNA binder in the metal(II) complexes is essential for observing efficient DNA cleavage activity. All the complexes are found to exhibit nuclease activity. Fig. 4 shows the result of gel electrophoretic separations of pBR322 DNA induced by an addition of metal(II) complexes in the presence of AH_2 (ascorbic acid). Under the same conditions, free AH_2 produces no cleavage of pBR322 DNA. During electrophoresis, while scission occurs on one strand (nicking), the supercoiled form relaxes to generate nicked form (Form II) [35]. When cleavage occurs on both the strands, a linear form (Form III) is generated which migrates between Forms I and II [36,37]. For this case, all supercoiled (Form I) DNAs are cleaved to form the mixture of Form II with the addition of the complexes. Since the nuclease

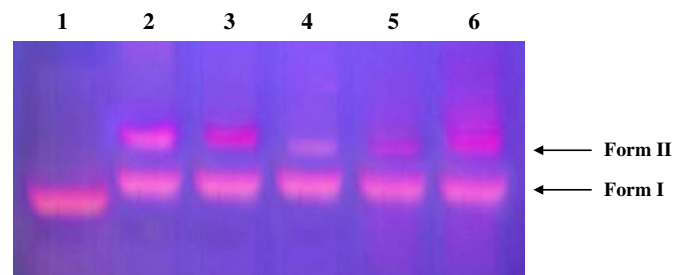


Fig. 4. Gel electrophoresis diagram showing the cleavage of pBR322 DNA (10 μM) by the Cu(II), Ni(II), Co(II) and Zn(II) complexes in a buffer containing 50 mM Tris-HCl and 50 mM NaCl in the presence of ascorbic acid (AH_2 , 10 μM) and DMSO (4 μL) at 37 $^\circ\text{C}$. Lane 1, DNA control; lane 2, DNA + ligand + AH_2 + DMSO (4 μL); lane 3, DNA + AH_2 + $[\text{CuL}(\text{ox})]\text{Cl}_2$ + DMSO (4 μL); lane 4, DNA + AH_2 + $[\text{NiL}(\text{ox})]\text{Cl}_2$ + DMSO (4 μL); lane 5, DNA + AH_2 + $[\text{CoL}(\text{ox})]\text{Cl}_2$ + DMSO (4 μL); lane 6, DNA + AH_2 + $[\text{ZnL}(\text{ox})]\text{Cl}_2$ + DMSO (4 μL).

efficiency of complexes is usually dependent on activators [38], the cleavage activity is significantly enhanced by the activator ascorbic acid. These phenomena imply that Cu(II), Co(II), Ni(II) and Zn(II) complexes induce intensively the cleavage of circular pBR322 DNA in the presence of AH_2 (Fig. 4). In order to clarify the cleavage mechanism of pBR322 DNA introduced by metal(II) complexes, the investigation has been carried out further on adding DMSO (hydroxyl radical scavenger). It reveals that Cu(II) and Zn(II) complexes promote the cleavage of pBR322 DNA more efficiently than Co(II) and Ni(II) complexes.

The synthesized ligand and its complexes have been tested for their *in vitro* antimicrobial activity. They were tested against the bacteria *Staphylococcus aureus*, *Pseudomonas aeruginosa*, *Escherichia coli*, *Bacillus subtilis*, and *Salmonella typhi* by paper disc method. The antibacterial activity of the newly synthesized compounds is presented in Table 3. The results indicate that the ligand exhibits moderate antibacterial activity with respect to the complexes against the same microorganisms under identical experimental conditions. Further, the antibacterial action of Schiff base ligand may be significantly enhanced on the presence of azomethine groups which have chelating properties. These properties may be used in metal transport across the bacterial membranes or to attach to the bacterial cells at a specific site from which it can interfere with their growth. Ligand exhibited MIC in the range of (16.7–15.4 $\mu\text{g}/\text{mL}$) against all the pathogens. The copper complex showed better antibacterial activity (MIC, 1.7–2.8 $\mu\text{g}/\text{mL}$) against the tested microorganisms than the other complexes which have MIC values in the range 3.1–4.7 $\mu\text{g}/\text{mL}$. It may be attributed to the atomic radius and the electronegativity of Cu(II) ion. Current studies reveal that the high atomic radius and electronegative metal ions in their metal complexes exhibit high antimicrobial activity. Higher electronegativity and large atomic radius decrease the effective positive charges on the metal complex molecules which facilitates their interaction with the highly sensitive cellular membranes towards the charged particle [39].

The Schiff base and its metal complexes were screened for their antifungal activity against *Aspergillus niger*, *Fusarium solani*, *Curvularia lunata*, *Rhizoctonia bataticola* and *Candida albicans*. The minimum inhibitory concentration (MIC) values of the investigated compounds are summarized in Table 4. A comparative study of MIC values of ligand (11.6–15.8 $\mu\text{g}/\text{mL}$) and its complexes (2.0–6.7 $\mu\text{g}/\text{mL}$) against all the fungi indicates that the metal complexes exhibit higher antifungal activity than the ligand. Such increased activity on metal chelation can be explained on the basis of Tweedy's chelation theory [40]. Chelation reduces the polarity of the metal ion considerably because of the partial sharing of its positive charge with the donor groups and also due to π -electron delocalization on the whole chelating ring. The lipids and polysaccharides are some important constituents of the cell wall and membranes which are preferred for metal ion interaction. Apart from this, the cell wall also contains many phosphates, carbonyl and cystenyl ligands which maintain the integrity of the membrane by acting as a diffusion barrier and also provide suitable sites for binding. Furthermore, increased lipophilicity enhances the penetration of the complexes into lipid membrane and blocking of the metal binding sites in the enzymes of microorganisms. These complexes also disturb the respiration process of the cell and thus block the synthesis of the proteins which

Table 3

The *in vitro* antibacterial activity of Schiff base and its metal complexes (MIC in $\mu\text{g}/\text{mL}$).

Complex	<i>S. aureus</i>	<i>P. aeruginosa</i>	<i>E. coli</i>	<i>B. subtilis</i>	<i>S. typhi</i>
[L]	16.7	15.4	16.3	15.7	14.6
$[\text{CuL}(\text{ox})]\text{Cl}_2$	1.7	2.4	2.3	2.6	2.8
$[\text{NiL}(\text{ox})]\text{Cl}_2$	3.2	3.6	2.9	3.1	3.4
$[\text{CoL}(\text{ox})]\text{Cl}_2$	3.7	3.3	3.9	4.2	4.6
$[\text{ZnL}(\text{ox})]\text{Cl}_2$	3.5	4.6	3.4	3.8	4.7
Ciprofloxacin ^a	1.7	1.9	2.0	1.8	2.4
DMF	–	–	–	–	–

^a Ciprofloxacin is used as the standard. MIC ($\mu\text{g}/\text{mL}$) minimum inhibitory concentration, i.e. the lowest concentration to completely inhibit the bacterial growth.

Table 4
The *in vitro* antifungal activity of Schiff base and its metal complexes MIC in $\mu\text{g/mL}$.

Complex	<i>A. niger</i>	<i>F. solani</i>	<i>C. lunata</i>	<i>R. bataicola</i>	<i>C. albicans</i>
[L]	12.7	13.4	15.2	11.6	15.8
[CuL(ox)]Cl ₂	2.0	2.1	2.8	3.4	4.6
[NiL(ox)]Cl ₂	4.3	3.6	4.7	4.5	5.4
[CoL(ox)]Cl ₂	5.1	4.9	5.8	6.4	6.7
[ZnL(ox)]Cl ₂	5.4	6.3	6.6	6.2	6.5
Fluconazol ^a	1.0	1.3	1.2	1.1	1.6
DMF	–	–	–	–	–

^a Fluconazol is used as the standard. MIC ($\mu\text{g/mL}$) minimum inhibitory concentration, i.e., the lowest concentration to completely inhibit the fungal growth.

restricts further growth of the organism. The data obtained from the results of antibacterial and antifungal studies reveal that all the complexes exhibit more biological activity against one or more bacterial and/or fungal strains as compared to the parent ligand, hence showing better results of bioactivities rather than their uncomplexed parent ligand [41].

In summary, the present work focuses on the synthesis and characterization of four tetradentate mixed ligand metal complexes and their interactions with DNA. Conductivity measurements show that all complexes have electrolytic nature (1:1 type) and contain two Cl anions out of the coordination sphere. Each metal has four-coordination and hence, the geometry can be described as square-planar. The cyclic voltammograms of the complexes recorded in DMF reveal quasi-reversible waves attributed to redox couples, characteristic for each metal complex. The DNA binding studies of the complexes using biophysical and spectroscopic techniques reveal that Cu(II) complex exhibits highest propensity for DNA binding and DNA binding mode is essentially non-covalent *via* intercalation. Meanwhile, the nature of the central metal ions also affects the intercalative ability order which is Cu(II) > Ni(II) > Co(II) > Zn(II). These results indicate that DNA might also serve as the primary target of these compounds; in addition, they should have many potential practical applications, just like the promising therapeutic drug candidates. Efforts are on to prepare compounds with this type of functionality and also to screen the compounds against few plant pathogenic fungal strains for their broad spectrum of activities. Based on the specific intercalation with DNA, efficient chemical nuclease activity is also observed for the complexes under physiological reaction conditions *via* oxidation damage pathway involving formation of active oxygen in the presence of the reducing agent (ascorbic acid). The research has led to the discovery of a series of compounds for further pharmacological investigation.

Acknowledgments

The authors express their heartfelt thanks to the Science & Engineering Research Board, New Delhi for financial assistance. They also express their gratitude to the College Managing Board, Principal and Head of the Department of Chemistry, VHNSN College, Virudhunagar for providing research facilities.

Appendix A. Supplementary material

Supplementary data to this article can be found online at <http://dx.doi.org/10.1016/j.inoche.2013.08.001>.

References

- P.C.A. Brujninx, P.J. Sadler, New trends for metal complexes with anticancer activity, *Curr. Opin. Chem. Biol.* 12 (2008) 197–206.
- T.W. Hambley, Metal-based therapeutics, *Science* 318 (2007) 1392–1393.
- C. Spinu, M. Pleniceanu, C. Tigae, Biologically active new Fe(II), Co(II), Ni(II), Cu(II), Zn(II) and Cd(II) complexes of N-(2-thienylmethylene)methanamine, *J. Serb. Chem. Soc.* 73 (2008) 415–421.
- W. Hung, C. Lin, Preparation, characterization and catalytic studies of magnesium complexes supported by NNO-tridentate Schiff-base ligands, *Inorg. Chem.* 48 (2009) 728–734.
- J.A. Ciller, C. Seoane, J.L. Soto, B. Yruetagoena, Synthesis of heterocyclic compounds. II. Schiff bases of ethyl 2-aminofurancarboxylates, *J. Heterocyclic Chem.* 23 (2009) 1583–1586.
- C.R. Bhattarjee, P. Goswami, P. Mondal, Synthesis, structural characterization and DFT studies of new mixed ligand iron(III) Schiff base complexes, *J. Coord. Chem.* 63 (2010) 2002–2011.
- C. Metcalfe, J.A. Thomas, Kinetically inert transition metal complexes that reversibly bind to DNA, *Chem. Soc. Rev.* 32 (2003) 215–224.
- X.B. Yang, Y. Huang, J.S. Zhang, S.K. Yuan, R.Q. Zeng, Synthesis, characterization and DNA interaction of copper (II) complexes with Schiff base ligands derived from 2-pyridinecarboxaldehyde and polyamines, *Inorg. Chem. Commun.* 13 (2010) 1421–1424.
- S. Rajalakshmi, T. Weyhermuller, A.J. Freddy, H.R. Vasanthi, B.U. Nair, Catalytic nanomedicine technology: copper complexes loaded on titania nanomaterials as cytotoxic agents of cancer cell, *Eur. J. Med. Chem.* 46 (2011) 608–617.
- K.B. Troev, A mini review on chemical fixation of CO₂: Absorption and catalytic conversion into cyclic carbonates, Elsevier Inc., Amsterdam, 2006. 253–284.
- I.A. Natchev, Liebigs, antimicrobial activities of a series of diphenyl (4'-(aryldiazanyl) biphényl-4-ylamino)(pyridin-3-yl)methylphosphonates, *Ann. Chem.* (1988) 861–867.
- K.M. Yager, C.M. Taylor, A.B. Smith, Asymmetric synthesis of alpha-aminophosphonates *via* diastereoselective addition of lithium diethylphosphite to chelating imines, *J. Am. Chem. Soc.* 116 (1994) 9377–9378.
- M.N. Dehkordi, A.K. Bordbar, P. Lincoln, V. Mirkhani, Spectroscopic study on the interaction of ct-DNA with manganese salen complex containing triphenyl phosphonium groups, *Spectrochim. Acta* 90A (2012) 50–54.
- C.R. Bhattarjee, P. Goswami, P. Mondal, Synthesis, reactivity, thermal, electrochemical and magnetic studies on iron(III) complexes of tetradentate Schiff base ligands, *Inorg. Chim. Acta* 387 (2012) 86–92.
- P.M. Reddy, R. Rohini, E.R. Krishna, A. Hu, V. Ravinder, Synthesis, spectral and antibacterial studies of copper(II) tetraaza macrocyclic complexes, *Int. J. Mol. Sci.* 13 (2012) 4982–4992.
- D.P. Singh, K. Kumar, C. Sharma, New 14-membered octaazamacrocyclic complexes: Synthesis, spectral, antibacterial and antifungal studies, *Eur. J. Med. Chem.* 45 (2010) 1230–1236.
- M. Zampakou, M. Akrivou, E.G. Andreadou, C.P. Raptopoulou, V. Psycharis, A.A. Pantazaki, G. Psomas, Structure, antimicrobial activity, DNA- and albumin-binding of manganese(II) complexes with the quinolone antimicrobial agents oxolinic acid and enrofloxacin, *J. Inorg. Biochem.* 121 (2013) 88–99.
- J.D. Moore, K.T. Sprott, P.R. Hanson, Conformationally constrained α -boc-aminophosphonates *via* transition metal-catalyzed/Curtius rearrangement strategies, *J. Org. Chem.* 67 (2002) 8123–8129.
- J. Huang, R. Chen, Synthesis and bioactivities of 1,3,2-benzodiazaphosphorin-2-carboxamide 2-oxides containing alpha-aminophosphonate groups, *Heteroat. Chem.* 11 (2000) 480–492.
- N. Raman, R. Jeyamurugan, R. Senthilkumar, B. Rajkapoor, Scott G. Franzblau, *In vivo* and *in vitro* evaluation of highly specific thiolate carrier group copper(II) and zinc(II) complexes on Ehrlich ascites carcinoma tumor model, *Eur. J. Med. Chem.* 45 (2010) 5438–5451.
- S.M. Abdallah, G.G. Mohamed, M.A. Zayed, M.S. Abou El-Ela, Spectroscopic study of molecular structures of novel Schiff base derived from *o*-phthalaldehyde and 2-aminophenol and its coordination compounds together with their biological activity, *Spectrochim. Acta* 73A (2009) 833–840.
- The Schiff base was synthesized by the direct condensation of *p*-chlorobenzaldehyde and *o*-phenylenediamine (2:1 M ratio), dissolved in ethanol. The resulting reaction mixture was refluxed for ca 3 h. The dark brown precipitate of Schiff base obtained was filtered, dried and finally preserved in a desiccator.
- Yield: 58%. Anal. Calc. for C₂₀H₁₄Cl₂N₂: C, 68.2; H, 3.9; N, 7.8; Found: C, 67.8; H, 3.6; N, 7.3 (%). IR (KBr pellet, cm⁻¹): 1631 ν (C=N); ¹H NMR (δ): (aromatic) 6.9–7.4 (m); (–HC=N) 8.6 (s); ¹³C NMR (δ): 118.2–122.5 (C₁ to C₃), 165.7 (C₄), 124.4 (C₅), 125.2 (C₆), 127.2 (C₇), 141.8 (C₈); λ_{max} (cm⁻¹) in DMF, 46,256 and 28,965.
- The Schiff base L (0.376 g, 1 mmol) dissolved in ethanol (25 mL) was added to an ethanolic solution (20 mL) of the metal chlorides (1 mmol) and oxalic acid (0.09 g, 1 mmol). The reaction mixture was refluxed for ca 3 h. The solution was evaporated to room temperature. The solid complexes separated were filtered, washed with ethanol and dried *in vacuo*.
- Yield: 53%. Anal. Calc. for C₂₂H₁₄Cl₂CuN₂O₄: Cu, 12.6; C, 52.3; H, 2.8; N, 5.5; Found: Cu, 12.2; C, 51.9; H, 2.7; N, 5.2 (%). IR (KBr pellet, cm⁻¹): 1614 ν (C=N); 1324 ν (C=O); 1686 ν (non-coordinated C=O in ox); 483 ν (M–N); 575 ν (M–O); Λ_{M} 10⁻³ (ohm⁻¹ cm² mol⁻¹) = 89.3; λ_{max} (cm⁻¹) in DMF, 40,345, 29,876 and 15,227; μ_{eff} (BM): 1.83.
- Yield: 49%. Anal. Calc. for C₂₂H₁₄Cl₂CoN₂O₄: Co, 11.8; C, 52.8; H, 2.8; N, 5.6; Found: Cu, 11.5; C, 52.4; H, 2.7; N, 5.2 (%). IR (KBr pellet, cm⁻¹): 1609 ν (C=N); 1321 ν (C=O); 1683 ν (non-coordinated C=O in ox); 474 ν (M=N); 567 ν (M=O); Λ_{M} 10⁻³ (ohm⁻¹ cm² mol⁻¹) = 78.6; λ_{max} (cm⁻¹) in DMF, 15,625 and 18,518 cm⁻¹; μ_{eff} (BM): 2.57.
- Yield: 50%. Anal. Calc. for C₂₂H₁₄Cl₂NiO₄: Ni, 11.7; C, 52.7; H, 2.8; N, 5.5; Found: Cu, 11.3; C, 52.2; H, 2.5; N, 5.2 (%). IR (KBr pellet, cm⁻¹): 1602 ν (C=N); 1317 ν (C=O); 1685 ν (non-coordinated C=O in ox); 462 ν (M–N); 561 ν (M–O); Λ_{M} 10⁻³ (ohm⁻¹ cm² mol⁻¹) = 74.8; λ_{max} (cm⁻¹) in DMF, 18,939 and 16,393; μ_{eff} (BM): diamagnetic.

- [28] Yield: 52%. Anal. Calc. for $C_{22}H_{14}Cl_2N_2O_4Zn$: Zn, 12.9; C, 52.2; H, 2.7; N, 5.5; Found: Zn, 12.4; C, 51.7; H, 2.6; N, 5.1 (%). IR (KBr pellet, cm^{-1}): 1605 $\nu(-C=N)$; 1312 $\nu(-C-O)$; 1684 $\nu(\text{non-coordinated } C=O \text{ in ox})$; 459 $\nu(M-N)$; 550 $\nu(M-O)$; 1H NMR (δ): (aromatic) 6.9–7.2 (m); ($-HC=N-$) 8.2 (s); ^{13}C NMR (δ): 117.6–121.8 (C_1 to C_3), 161.2 (C_4), 124.2 (C_5), 124.9 (C_6), 126.8 (C_7), 141.6 (C_8), 167.6 (C_9); $\Lambda_M 10^{-3} (\text{ohm}^{-1} \text{cm}^2 \text{mol}^{-1}) = 67.2$; $\lambda_{\text{max}} (\text{cm}^{-1})$ in DMF, 27,397 and 26,917; μ_{eff} (BM): diamagnetic.
- [29] Q. Wu, C. Fan, T. Chen, C. Liu, W. Mei, S. Chen, B. Wang, Y. Chen, W. Zheng, Microwave-assisted synthesis of arene ruthenium(II) complexes that induce S-phase arrest in cancer cells by DNA damage-mediated p53 phosphorylation, *Eur. J. Med. Chem.* 63 (2013) 57–63.
- [30] J.B. Lepecc, C. Paoletti, A fluorescent complex between ethidium bromide and nucleic acids. Physical-chemical characterization, *J. Mol. Biol.* 27 (1967) 87–106.
- [31] A.E. Friedman, J.C. Chambron, J.P. Sauvage, N.J. Turro, J.K. Barton, Molecular "Light Switch" for DNA: $Ru(\text{bpy})_2(\text{dppz})_2^+$, *J. Am. Chem. Soc.* 112 (1990) 4960–4962.
- [32] L.-Z. Li, C. Zhao, T. Xu, H.-W. Ji, Y.-H. Yu, G.-O. Guo, H. Chao, Synthesis, crystal structure and nuclease activity of a Schiff base copper(II) complex, *J. Inorg. Biochem.* 99 (2005) 1076–1082.
- [33] S. Satyanarayana, J.C. Dabroniak, J.B. Chaires, Neither delta- nor lambda-delta-tris(phenanthroline)ruthenium(II) binds to DNA by classical intercalation, *Biochemistry* 31 (1992) 9319–9324.
- [34] J. Sun, S. Wu, Y. An, J. Liu, F. Gao, L.N. Ji, Z.W. Mao, Synthesis, crystal structure and DNA-binding properties of ruthenium(II) polypyridyl complexes with dicationic 2,2'-dipyridyl derivatives as ligands, *Polyhedron* 27 (2008) 2845–2850.
- [35] M.S. Melvin, J.T. Tomlinson, G.R. Saluta, G.L. Kucera, N. Lindquist, R.A. Manderville, *J. Am. Chem. Soc.* 122 (2000) 6333–6334.
- [36] Y. Jung, S.J. Lippard, Direct cellular responses to platinum-induced DNA damage, *Chem. Rev.* 107 (2007) 1387–1407.
- [37] X. Dong, X. Wang, M. Lin, H. Sun, X. Yang, Z. Guo, Promotive effect of the platinum moiety on the DNA cleavage activity of copper-based artificial nucleases, *Inorg. Chem.* 49 (2010) 2541–2549.
- [38] C.A. Detmer III, F.V. Pamatong, J.R. Bocarsly, Molecular recognition effects in metal complex mediated double-strand cleavage of DNA: Reactivity and binding studies with model substrates, *Inorg. Chem.* 36 (1997) 3676–3682.
- [39] N.A. Negma, M.F. Zakia, M.A.I. Salem, Cationic Schiff base amphiphiles and their metal complexes: Surface and biocidal activities against bacteria and fungi, *Colloids Surf. B: Biointerfaces* 77 (2010) 96–103.
- [40] R. Ramesh, S.J. Maheswaran, Synthesis, spectra, dioxygen affinity and antifungal activity of Ru(II) Schiff base complexes, *J. Inorg. Biochem.* 96 (2003) 457–462.
- [41] Z.H. Chohan, C.T. Supuran, Structure and biological properties of first row d-transition metal complexes with N-substituted sulfonamides, *J. Enzym. Inhib. Med. Chem.* 23 (2008) 240–251.